HHS Public Access

Author manuscript

Nanomedicine. Author manuscript; available in PMC 2016 July 27.

Published in final edited form as:

Nanomedicine. 2014 April ; 10(3): 619–627. doi:10.1016/j.nano.2013.09.004.

Theranostic Immunoliposomes for Osteoarthritis

Hongsik Cho, Ph.D.[1,2,3], **Richard Magid, Ph.D.**[1], **Delia C. Danila, Ph.D.**[4], **Tamra Hunsaker, Ph.D.**[4], **Eugene Pinkhassik, Ph.D.**[4], and **Karen A Hasty, Ph.D.**[1,2,3,¶]

[1]University of Tennessee Health Science Center, Memphis, TN

[2]Campbell Clinnic, Memphis, TN

[3]Veterans Affairs Medical Center, Memphis, TN

[4]University of Memphis, Memphis, TN

Abstract

Although there have been substantial advancements in the treatment of inflammatory arthritis, treatments for osteoarthritis (OA) have lagged and currently are primarily palliative until joints become totally dysfunctional and prosthetic replacement is needed. One obstacle for developing a preventive therapy for OA is the lack of good tools for efficiently diagnosing the disease and monitoring its progression during the early stages when the effect of therapeutic drugs or biologics are most likely to be effective. We have developed near infrared immuno-liposomes conjugated with type II collagen antibody for diagnosis and treatment of early OA. These immuno-liposomes bind to damaged but not normal cartilage. Utilizing these reagents, we can quantitate exposure of type II collagen during cartilage degradation in individual joints in vivo in a guinea pig. Immuno-liposomes could be used to determine the effectiveness of therapeutic interventions in small animals as well as vehicles for localized drug delivery to OA chondrocytes.

Graphical Abstract: Schematic diagram of antibody targeted immunoliposomes binding onto damaged cartilage

Antibodies to type II collagen are normally blocked from binding to the surface of the articular cartilage. Proteolytic enzymes secreted by resident chondrocytes, synoviocytes or infiltrating leukocytes degrade the surface proteins and allow access of the antibodies to the type II collagen fibrillar network within.

[¶]To whom correspondence should be addressed: Karen A. Hasty, Ph.D, Department of Orthopaedic Surgery, University of Tennessee, Research 151 VAMC, 1030 Jefferson Ave, Memphis TN 38138 USA, Phone: 1-901-523-8990 (ext 6175), Fax: 1-901-577-7273, khasty@uthsc.edu.

We have no conflicts of interest to disclose.

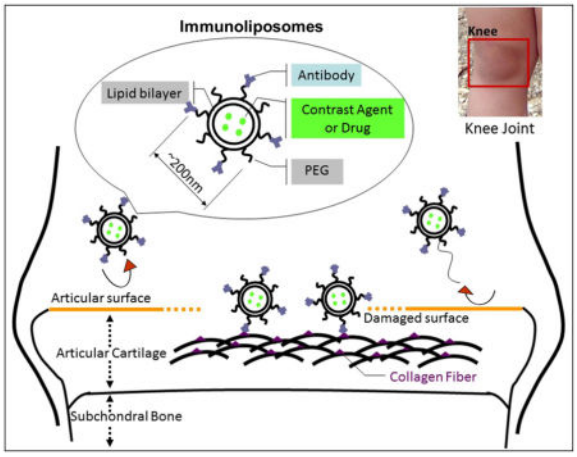

Keywords

Immuno-liposomes (ILs); Osteoarthritis (OA); type II collagen(CII); theranostic (therapeutic and diagnostic); extracelluar matrix(ECM); near-infrared (NIR) fluorescent

BACKGROUND

Arthritis is a leading cause for disability in the nation, and osteoarthritis (OA) is the most prevalent arthritis. Initially with OA, extracellular matrix (ECM) and chondrocytes are progressively eroded from the superficial surface of the articular cartilage. With time, the lesion gradually deepens until the underlying subchondral bone is exposed. In the knee, this typically begins in the medial condyles, areas of cartilage subjected to the greatest mechanical stress, and the time course of erosion is accelerated by factors such as obesity, repetitive stress and aging [1, 2, 3]. Degradation of the cartilage matrix is facilitated by proteinases that deteriorate the components of the ECM that are produced by the chondrocytes themselves or exogenously produced by synoviocytes or infiltrating leukocytes. Following proteolysis, the loss of proteoglycans and other proteins from the surface exposes type II collagen fibrils which become accessible to type II collagen (CII) antibodies [4, 5].

Pharmacological treatment of this OA is currently only palliative until advanced joint disability necessitates prosthetic replacement. Because OA begins as a focal lesion that slowly progresses, there may be opportunity for early intervention [3]. However, there are obstacles in developing therapies for this disease. Monitoring disease progression quantitatively is difficult. Cartilage is radiolucent by conventional x-ray, so efficacy of treatment is difficult to evaluate without expensive MRI measurements that may have to span over a decade [6, 7]. Animal models have a more rapid progression of disease, but histopathological evaluation is an endpoint analysis and is tedious and expensive [8, 9]. Spontaneous OA models have considerable variability in incidence, severity and time course of development requiring large numbers of animals [10, 11].

Drug delivery by antibody-conjugated liposomes, immuno-liposomes, represents a technology that has been applied to the targeting of specific sites of drug action, such as brain, lung, cancer cells or cells of the immune system [12, 13, 14, 15, 16]. The field of immuno-liposomes has been continuously developing to provide various physical and biochemical formulations with a high degree of target specificity [17, 18, 19]. Unmodified liposomes conjugated to antibody are phagocytosed by the reticulo-endothelial system (RES), so lipids are modified by the addition of polyethylene glycol (PEG) to increase their circulating half-life. Pendant-type PEG immuno-liposomes carry antibodies or their fragments at the distal ends of the PEG chains. This type of liposome has been shown to exhibit higher binding efficiency to target tissues, and this is the type of liposome that this study has employed [20, 21].

In this project, we have investigated if differential binding of type II collagen antibodies to the surface of damaged articular cartilage might be used as a sensitive and quantitative indicator of cartilage damage as well as target immuno-liposomes for potential delivery of imaging and therapeutic agents.

MATERIALS AND METHODS

Animal and in vivo test

Two different age groups (3–5 month and 1–2 years old) of Dunkin-Hartley (DH, osteoarthritic) guinea pigs (n=18 for each age group) were used in these experiments. The spontaneous model of OA in DH-guinea pigs shares many features of human OA including correlation with obesity, aging and increased severity in weight bearing areas of the articular cartilage [8]. 100μl of immunoliposomes that contains near infrared-emitting dye, Xenofluor 750 (0.38μmole, Caliper Life Science, Hopkinton, MA) and labeled with monoclonal anti-collagen type II antibody (MAbCII, 10μg) was intravenously injected into the DH-guinea pigs of 3–5 months (young) or 1–2 year (old) of age (n=12 for each age group). The control group received a labeled irrelevant monoclonal mouse IgG antibody of the same subclass (MAbCon) (n=3 for each age group). At 24 hours post-injection, animals were imaged by IVIS scanning (IVIS® Lumina II System, Caliper Life Science, Hopkinton, MA) with an Indocyanine Green (ICG) filter set (excitation 710–760nm, emission 810–875 nm) and the fluorescence remaining in the joint was quantitated. Both knees were dissected, fixed the femoral and tibial portions for histopathology after re-scanned with IVIS. All animal experiments were performed according to approved protocols and experimental procedures at the University of Tennessee Health Sciences Center.

Source of tissues and cell isolation for in vitro test

The articular cartilages used in this investigation were obtained from knee joints and femoral heads from 1–2 week-old pigs. All tissues were taken from the cartilages of healthy pigs freshly sacrificed for other experiments according to approved protocols and experimental procedures at the University of Tennessee Health Sciences Center. Cells from articular cartilage tissue were isolated by 1–2 hours digestion at 37°C in 0.05% Pronase (Roche Diagnostics Corp., Indianapolis, IN), followed by overnight digestion at 37°C in 0.2% collagenase (Worthington Biochemical Corp., Lakewood, NJ) using modified F-12K

medium (Invitrogen, Grand Island, NY) with 5% fetal calf serum (FCS, Atlanta Biologicals, Norcross, GA), 4.8 mM $CaCl_2$ and 40 mM HEPES buffer (Sigma, St. Louis, MO). The cells were washed in F-12K medium and plated (1.5×10^4 cells/cm^2) onto culture plates. Cells were cultured at 37°C in a humidified atmosphere of 5% CO_2 in air, and the medium supplemented with 10% fetal calf serum, streptomycin (50 μg/ml), penicillin G (50 IU/ml), L-glutamine (2mM) and L-ascorbic acid (50 μg/ml). The medium was changed every other day.

Monoclonal mouse IgG and anti-collagen II antibody

The generation and characterization of the anti-collagen type II monoclonal antibodies (MAbCII) is described in *Terato et al.* [22]. An immunoassay was performed to assess binding and specificity of these antibodies for type II collagen purified from guinea pig knee cartilage. The results showedth at only one of them, MAbCII (D8), has strong immuno-reactivity to the guinea pig collagen, so D8 was chosen for use in this study. For these studies, that purified monoclonal antibody was obtained from the VA Program Project Scientific Coreat the VA Medical Center (Memphis, TN). The monoclonal mouse IgG_{2A} antibody (MAbCon) of the same subclass from R&D Systems (Mouse IgG2A Isotype Control, Clone 20102, Minneapolis, MN) was used for a control antibody.

Liposome synthesis and antibody coupling

The method of liposome synthesis and antibody coupling was adapted from *Huwyler et al.*[23,24,25,26]. All lipids were purchased from Avanti Polar Lipids (Alabaster, AL) as pure powders, and dissolved in 2:1 chloroform:methanol. A lipid film was prepared by mixing 5.2 μmol 1,2-dioleoyl-sn-glycero-3-phosphocholine (DOPC, Avanti Polar Lipids, AL), 4.5 μmol cholesterol, 0.3 μmol 1,2-distearoyl-sn-glycero-3-phosphoethanolamine-N-[methoxy(polyethylene glycol)-2000] (DSPE-$PEG_{2000,}$ Avanti Polar Lipids, AL), and 0.015 μmol 1,2-distearoyl-sn-glycero-3-phosphoethanolamine-N-[maleimide (polyethylene glycol) 2000] (DSPE-PEG_{2000}-maleimide, Avanti Polar Lipids, AL). This lipid mixture was initially dried under an argon stream for 30 min, and then further dried under vacuum for 30 min. The lipid film was rehydrated by vortexing with PBS, which was supplemented with 0.8 ml of horseradish peroxidase (HRP, 10mg/ml) or fluorescent dye for liposome encapsulation. The rehydrated lipids were repeatedly extruded through a membrane that has a 200nm diameter pore size (Millipore, MA) to generate 200 nm single-walled liposomes [17, 28, 29]. The extruded liposomes were separated from the free molecules using a Sepharose CL-4B (Sigma-Aldrich, MO) size exclusion column prior to coupling the antibody to the liposome. The purified liposomes were then mixed with the freshly thiolated antibody, and the reaction was allowed to proceed for 16 hours at room temperature. The next day, the reaction mixture was again chromatographed on a Sepharose column to separate the free antibody from the coupled liposomes.

Collagen II ELISA

For ELISA, 96-well plates were coated with 1 μg of denatured collagen II per well, and then blocked with 1% BSA. For experiments in which the samples were pre-incubated with a known concentration of soluble collagen, this step was performed in BSA-blocked wells without surface-bound collagen. All samples, whether liposomes or free antibody, were

incubated at 4°C overnight, followed by a PBS wash. For the detection of bound antibody, an alkaline phosphatase coupled anti-mouse IgG secondary antibody was used (1:2,000 dilution in PBS-T;10 mM phosphate buffer pH 7.4, 150 mM NaCl, 0.05% Tween 20). For the detection of bound liposomes which contained HRP, the p-nitrophenyl phosphate (PNPP, Thermo Scientific, IL) substrate at 405 nm or the 3,3′ tetramethylbenzidine (TMB) substrate (1-Step TM Turbo TMB-ELISA; Pierce, IL) were used to generate a colored substrate. The TMB has an absorption maximum at 285 nm before oxidation. After oxidation and the addition of the stop solution (1M H_2SO_4), the yellow solution can be measured at 450 nm.

Localization of immuno-liposomes onto OA chondrocytes

To determine if the immuno-liposome localize to the pericellular extracellular matrix (ECM) of cultured chondrocytes, the culture medium was replaced with 500 μl of PBS containing immuno-liposomes, or liposomes alone as a control, and incubated for 1 h at 37°C. Excess liposomes were removed by PBS washes prior to collection of morphological images. After washing, the cells were fixed with 10% formalin (Sigma-Aldrich, MO) for fluorescence microscopy or 25% glutaraldehyde (Tousimis, MD) for SEM analysis, respectively. The localization of immunoliposomes on the chondrocytes were visualized by scanning electron microscopy (SEM) and fluorescence microscopy (Cytoviva™, AL).

Proteolytic treatment of normal articular cartilage and binding to liposomes

To investigate the localization of immunoliposomes encapsulating HRP to damaged cartilage, explants from normal porcine cartilage were used. To create a proteolytic damage, the experimental groups was treated with 0.5% trypsin-EDTA (Gibco, PA) for 30 min at 37°C to mimic arthritic-like cartilage and the control group was treated with PBS. Both groups were treated with immunoliposomes encapsulating HRP or liposomes with HRP not coupled to antibody, respectively. Following several rinses in PBS, non-specific binding was blocked by incubating the tissue in 5% goat serum (in PBS) for 60 minutes at room temperature. All cartilage tissues were stained with diaminobenzidine (DAB) substrate (Vector, CA) for detection of liposomes after re-punching out the explant core with a 4mm biopsy punch (Miltex Inc; York PA). For the quantitative detection of bound immunoliposomes containing HRP, the 2,2′-azino-bis (3-Ethylbenzthiazoline-6-Sulfonic acid) substrate (ABTS; Vector, CA) was used to generate a soluble colored substrate measured at 405 nm. The preparation of the solution and procedure were done following the company's instructions.

Statistics

All experiments were performed independently at least three times. Student's t-tests were performed to determine statistical significance.

RESULTS

Characterization of immuno-liposomes

After preparation, the size distribution and sample consistency were verified using transmission electron microscopy (TEM; JEM1200EX II, JEOL USA Inc, MA) (Figure 1, C) and dynamic light scattering (DLS) (Figure 1, B). To determine size distribution using

TEM, the liposomes were negatively stained by phosphotungstic acid (PTA). In the DLS (Malvern, UK) analysis, the extrusion of multilamellar vesicles through polycarbonate track etched filters with uniform cylindrical 200 nm pores results in uniformly sized liposomes (average diameter is 200 nm) (Figure 1, B). By TEM, the sizes of prepared liposomes were uniformly in the range of 150–250 nm. Liposomes were predominantly unilamellar with a fraction of them having two of three lamellae (Figure 1, C).

The specific binding of MabCII labeled liposomes was tested using an ELISA technique on plates coated with type I collagen (CI) and type II collagen (CII). Following characterization of monoclonal antibody for type II collagen, empty liposomes were prepared according to the method described above, including the coupling of MabCII. For the control liposomes, the thiolation of the antibody was omitted. In both groups tested, the liposomes eluted from the column in fractions #6–8, and only the coupled liposomes were observed to bind collagen II in an ELISA format. The bulk of the antibody was detected as free antibody (fractions #14+). Importantly, the elution of the free antibody was separated from the liposome elution (Supplementary Information S1).

To determine the kinetics for binding of the antibody-coupled liposomes, the liposomes were pre-incubated with a known concentration of CII for 1 hour at room temperature. They were then bound to an ELISA plate coated with CII. Bound antibody was detected with an alkaline phosphatase coupled secondary antibody, using a PNPP substrate. The level of inhibition was calculated compared to the uninhibited liposomes. An inhibition curve with known concentrations of soluble collagen II was determined. This curve, when plotted semi-logarithmically, exhibited excellent linearity over the range from 125ng/mL to 20μg/mL. Using the calculated regression curve, we determined that the level of free collagen required for 50% inhibition of antibody binding (K_d) was 1.7μg/mL, or 18nmol/L (Figure 1, A). The inhibition of binding (compared to the control with no collagen) was calculated using 95kD as the molecular weight of a single collagen II chain.

In vitro test of immuno-liposomes

It is critical that the immuno-liposomes bind to the exposed type II collagen in the ECM of chondrocytes, while liposomes that are not coupled to antibody or coupled to an irrelevant antibody do not. Cultured articular chondrocytes were tested for studies of the type II collagen antibody-labeled liposomes synthesized with HRP. Primary articular chondrocytes from pig were cultured in vitro for 3–4 days to allow matrix formation, then were washed with serum-free medium and incubated with 500 ul of PBS containing immuno-liposomes or liposomes alone as a control for 1 h at 37°C. Excess liposomes were removed by PBS washes prior to collection of morphological images. After washing, the cells were fixed with 10% formalin (Sigma-Aldrich, MO) for fluorescence microscopy or 25% glutaraldehyde (Tousimis, MD) for Scanning Electron Microscopy (SEM; FEI XL, FEI Corp, OR) analysis, respectively. Figure 2(A~D) shows a series of SEM and fluorescent microscopy images of chondrocytes incubated with peroxidase-filled liposomes and incubated with DAB substrate. As shown, SEM and fluorescent microscopy shows that only type II collagen antibody (MAbCII)-coupled liposomes significantly bound to the ECM of the chondrocytes (white

particles on Figure 2, B and D/brownish stain on Figure 2, F) while unconjugated liposome controls showed no binding (Figure 2, A, C and E).

Type II collagen in normal cartilage is not available for binding but it can be unmasked when the surface of the cartilage is treated with proteases [5]. To investigate the localization of immuno-liposomes encapsulating horseradish peroxide (HRP) to damaged cartilage in vitro, full thickness explants from porcine normal articular cartilage were used. Some explants were briefly incubated with trypsin to proteolytically digest the proteoglycans from the surface while the control explants were treated with PBS. Both groups were incubated with immuno-liposomes encapsulating HRP or control liposomes that were not coupled to antibody. All cartilage tissues were stained with diaminobenzidine (DAB) for detection of liposomes with HRP (Figure 3). This data was confirmed and quantitated using an ABTS substrate (Supplementary Information S2). Only the MAbCII coupled immuno-liposomes bound to the damaged cartilage (Figure 3, C); normal cartilage showed minimal binding of immuno-liposomes. Liposomes alone (Control Liposome)did not bind to either damaged or normal cartilage.

In vivo test of immunoliposomes

To test the ability of the immuno-liposomes to localize *in vivo* to degraded cartilage, we labeled the immuno-nanosomes by encapsulation of a near-infrared (NIR) dye, Xenofluor™750, and injected them in young (5–7 month old) and older (1–2 year) DH-guinea pigs. This strain of guinea pigs develops spontaneous arthritis upon aging. As controls, NIR dye-loaded liposomes were coupled to an isotype control antibody (MAbCon). The NIR dye was quantitatively visualized *in vivo* at 24 hours post-injection using an IVIS. In our previous experiments aimed at optimizing imaging time, live images of fluorescence distribution show that fluorescent antibody can be found in the synovial cavity within 3 hours of injection regardless of specificity. However, IVIS imaging shows that after 24 hrs, the fluorescence will no longer be found in the joint space if the fluorescent antibody is not targeted to CII. The fluorescence signal intensity of immuno-liposomes reaches its maximum at the peak of disease activity. Joints were also dissected at that time and imaged separately. The knees of guinea pigs showed a significant difference between those young and old groups injected with NIR-MAbCII lipoosomes (Figure 4, A and B). In the old group with NIR-MAbCII liposome showed a high degree of binding and exhibited fluorescence corresponding to histopathological joint degradation (Figure 4, E and G). As shown in Figure 4, this binding is proportional to the extent of cartilage damage in the joint. Liposomes conjugated to a control antibody showed minimal binding (Supplementary Information S3). IVIS imaging of the dissected tissue surrounding the joint in both young and old samples showed no soft tissue fluorescence (Supplementary Information S3). Binding of the NIR-MAbCII liposomes was principally to the medial condyles in the old animals (Figure 4, C). Uptake of fluorescent immuno-liposomes by liver and spleen tissue could be seen visually. Minimal uptake was seen in the kidney at 24 hours. However, we saw visual confirmation of accumulation of immuno-liposomes in the bladder as well as in the urine collected after micturition indicating renal excretion.

Histopathology of the joint was also performed to confirm and quantitate cartilage degradation. As expected, the articular cartilage in the young pig had limited degradation (Figure 4, D and F) while older joints displayed osteoarthritis with characteristic cartilage damage (Figure 4, F and G). These sections were then graded by an observer using a modified Mankin scale [30, 31]. The older animals scored 4–5 with loss of superficial cartilage layer, surface irregularities, with some clefts into the middle zone and decreased chondrocytes within the tissue. Both the medial and lateral condyles showed more severe degenerative changes in the older animals, while those of the young animals showed only confined regions of superficial cell loss corresponding to a modified Mankin score of 1–2 (confirmed by IVIS scanning in Figure 4, C).. The right knees of older animals showed 4–5 times the fluorescence seen in younger animals. (Figure 4, H).

DISCUSSION

In this study, we used the 200nm size of pendant-type PEG immuno-liposomes carrying CII antibodies at the distal ends of the PEG-maleimide chains. This type of liposome has been shown to exhibit higher binding efficiency to target tissues, and this is the type of liposome that this study has employed [20, 21]. In addition to the chemical composition, the physical size of the liposome is also a contributory factor to its circulation time [32, 33, 34]. Smaller liposomes, nanosomes, ranging in size from 70 to 300 nm better avoid immune surveillance. Liu et al. have reported that liposomes with a diameter less than 70 nm are rapidly removed from the circulation and mainly accumulated in the liver [35, 36]. They also reported that splenic uptake becomes predominant when the liposome diameter was 300 nm or greater [33, 37, 38, 39].

CII is the one of major components of the ECM of hyaline cartilage. However, in normal cartilage, it is not available for binding to type II collagen antibodies unless some proteolysis at the articular surface has occurred [5, 12]. This is probably due to proteolytic digestion and loss of proteoglycans, as increased CII antibody binding is also seen with a brief extraction of the intact cartilage surface with a strong chaotropic agent. This suggests that the protective material is non-covalently bound to the surface macromolecules [30]. Exposure of CII in articular cartilage, therefore, may be a more direct reflection of initial cartilage degradation in OA than either synovial fluid, serum or urine markers [12, 40]. Previously, we characterized mouse monoclonal antibodies to type II collagen for studies of passive transfer of autoimmune arthritis in which a cocktail of different monoclonal antibodies localize to articular cartilage and bind complement initiating inflammatory arthritis [22]. In this study, we have selected only one monoclonal antibody for our use. One antibody does not bind complement, a process that takes close proximity of several antibodies, and does not initiate arthritis.

As shown in Figure 4, specific binding of NIR-MAbCII liposomes to articular cartilage in knee joints was seen with IVIS imaging in older DH-guinea pigs. This strain is known to show increased incidence of spontaneous OA with aging with erosions of articular cartilage [11]. We predicted that increased cartilage proteolysis in OA would unmask type II collagen, thus increasing availability for binding of liposomes conjugated to antibody for type II collagen. Histopathology confirmed that the joints with higher binding of liposomes

also had increased levels of articular cartilage degradation. Comparison of IVIS imaging with histopathological data shows that the binding of liposomes is localized to the areas of OA damage. Quantitation of regions of interests (ROI) by IVIS software analyses and histopathological comparisons indicate that the amount of liposome binding is proportional to the extent of cartilage degradation. Furthermore, in older guinea pigs group, we injected two different types of liposomes which are liposome only and MAbCon immuno-liposome to test possibility of nonspecific bind. This might be due to nonspecific phagocytosis by activated macrophages, or due to liposome pooled at the interstitial space because of increased vascular permeability at the inflammation tissues. In our previously study, however, we did not find nonspecific bind cause of inflammation in both of liposome only and MAbCII immuno-liposome injected group. (Supplementary Information S3)

We believe that future studies with MAbCII targeted immuno-liposomes will be able to not only detect, but provide a quantitative measurement for the stage of OA. Encapsulation of drugs or cytokines inside the liposomes should prove a valuable method for delivery of localized treatment to early OA lesions. With our current study, we have investigated and exhibited that MAbCII conjugated to a liposome can gain access and bind to damaged cartilage present in OA. Through this process, it is evident that these immuno-liposomes could prove beneficial to early diagnosis and treatment at any stage of OA. The ability to identify early damage to the articular surface and specifically direct biological agents to OA cartilage offers a new paradigm for treating early osteoarthritis with theranostic (therapeutic and diagnostic) liposomes [41]. Employing these MAbCII antibody conjugated liposomes addresses the two major impediments in developing treatment of OA. First, this method permits avoidance of expensive imaging of cartilage and secondly, it provides a targeted means of transporting therapeutic agents for localized delivery to the OA chondrocyte. New therapies with growth factors and biologics showing efficacy in vitro may have unintended consequences for adjacent soft tissues when intraarticularly injected [38, 42]. For example, while transforming growth factor (TGF) shows great promise for reducing matrix metalloproteinase (MMP) expression of chondrocytes from the OA lesion [43, 44, 45, 46], it cannot be directly injected into the joint as TGF has been shown to be responsible for osteophyte formation in synovial tissues [47, 48]. Targeted delivery of TGF to the OA chondrocyte could possibly circumvent this undesirable side effect. Furthermore, employment of theranostic immuno-liposomes during drug evaluation does not necessitate sacrifice of animal subjects allowing serial measurements in the same animal.

In conclusion, we demonstrated selective binding of liposomes bearing CII antibodies onto OA lesions in vivo. These liposomes are delivered systemically and are sufficiently stable to localize in the joints following an IV injection. The amount of binding is proportional to the extent of the damage of cartilage. This technology has the potential for overcoming the obstacles of current methods for diagnosis and treatment of OA. It can be applied to early diagnosis, to serial measurement of disease progression in individual joints and for determining the effectiveness of therapeutic interventions in small animals. Our preliminary data shows its usefulness for arthritis detection in rodents. While we have incorporated NIR dyes into liposomes bearing CII antibodies for in vivo monitoring of small animals, the technique can be easily modified for quantitative measurements with clinically proven and measurable radiopharmacological compounds, such as technetium, allowing a relatively

inexpensive (compared to MRI) evaluation in patients using existing clinical protocols and available equipment.

Supplementary Material

Refer to Web version on PubMed Central for supplementary material.

Acknowledgments

This research was supported by a VA Merit Review award from Department of Veterans Affairs, CTSI from the UTHSC and R21 from NIH (KAH) and also the Arthritis Foundation Fellowship Award (H. Cho).

This work supported with resources and the use facilities at the Veterans Affairs Medical Center (VAMC) at Memphis TN USA. This research was supported by a VA Merit Review award from Department of Veterans Affairs, R21from NIH (AR060408) and CTSI from the UTHSC (Karen A. Hasty) and also the Arthritis Foundation Fellowship Award (H. Cho).

References

1. Aspden RM. Osteoarthritis: a problem of growth not decay? Rheumatology. 2008; 47:1452–1460. [PubMed: 18495820]
2. Bitton R. The economic burden of Osteoarthritis. Am J Manag Care. 2009; 15:230–235.
3. Wieland HA, Michaelis M, Kirschbaum BJ, Rudolphi KA. Osteoarthritis; An untreatable disease? Nature Review. 2005; 4:331–344.
4. Elsaid KA, Chichester CO. Collagen markers in early arthritic diseases. Clinica Chimica Acta. 2006; 365:68–77.
5. Jasin HE, Noyori K, Takagi T, Taurog JD. Characteristics of anti-type II collagen antibody binding to articular cartilage. Arthritis Rheum. 1993; 36(5):651–9. [PubMed: 8489543]
6. Quatman CE, Hettrich CM, Schmitt LC, Spindler KP. The Clinical Utility and Diagnostic Performance of Magnetic Resonance Imaging for Identification of Early and Advanced Knee Osteoarthritis: A Systematic Review. Am J Sports Med. 2011; 39:1557–1568. [PubMed: 21730207]
7. Leblond F, Davis SC, Valdes PA, Pogue BW. Pre-clinical whole-body fluorescence imaging: Review of instruments, methods and applications. J Photochem Photobiol B. 2010; 98(1):77–94. [PubMed: 20031443]
8. Ameye LG, Young MF. Animal models of osteoarthritis: lessons learned while seeking the “Holy Grail”. Curr Opin Rheumatol. 2006; 18(5):537–47. [PubMed: 16896297]
9. Bendele AM. Animal models of osteoarthritis. J Musculoskel Neuron Interact. 2001; 1(4):363–376.
10. Bendele AM. Animal models of osteoarthritis in an era of molecular biology. J Musculoskel Neuron Interact. 2002; 2(6):501–503.
11. Huebner JL, Hanes MA, Beekman B, Tekoppele JM, Kraus VB. A comparative analysis of bone and cartilage metabolism in two strains of guinea-pig with varying degrees of naturally *occurring osteoarthritis*. Osteoarthritis and Cartilage. 2002; 10:758–767. [PubMed: 12359161]
12. Hollander AP, Heathfield TF, Webber C, Iwata Y, Boume R, Rorabeck C, Poole R. Increased damage to type II collagen in osteoarthritic articular cartilage detected by a new immunoassay. J Clin Invest. 1994; 93:1722–1732. [PubMed: 7512992]
13. Hovinga S, Seynhaevea ALB, Tiela STV, Eggermonta AMM, Hagena TLM. Addition of low-dose tumor necrosis factor-a to systemic treatment with STEALTH liposomal doxorubicin (Doxil) improved anti-tumor activity in osteosarcoma-bearing rats. Anti-Cancer Drugs. 2005; 16(6):667–674. [PubMed: 15930896]
14. Noyori K, Koshino T, Takagi T, Okamoto R, Jasin HE. Binding characteristics of antitype II collagen antibody to the surface of diseased human cartilage as a probe for tissue damage. The J of Rheumatology. 1994; 21(2):293–296.

15. O'Connell JP, Campbell RL, Fleming BM, Mercolino TJ, Jonhson MD, McLaurin DA. A highly sensitive immunoassay system involving antibody-coated tubes and liposome-entrapped dye. Clin Chem. 1985; 31(9):1424–1426. [PubMed: 4028391]
16. Scott RC, Wang B, Nallamothu R, Pattillo CB, Perez-Liz G, Issekutz A, Valle LD, Wood GC, Kiani MF. Targeted delivery of antibody conjugated liposomal drug carriers to rat myocardial infarction. Biotech and Bioeng. 2007; 96(4):795–802.
17. Ishida T, Iden DL, Allen TM. A combinatorial approach to producing sterically stabilized (stealth) Immunoliposomal drugs. FEBS Letters. 1999; 460:129–133. [PubMed: 10571074]
18. Leserman LD, Machy P, Barbet J. Cell-specific drug transfer from liposomes bearing monoclonal antibodies. Nature. 1981; 293(5829):226–228. [PubMed: 7278980]
19. Maruyama K, Takizawa T, Takahashi N, Tagawa T, Nagaike K, Iwatsuru M. Targeting efficiency of PEG-Immunoliposome-conjugated antibodies at PEG terminals. Advanced Drug Delivery Reviews. 1997; 24:235–242.
20. Lasic D, Papahadjopoulos D. Liposomes revisited . Science. 1995; 267(5202):1275–1276. [PubMed: 7871422]
21. Maruyama K. PEG-Immunoliposome. Bioscience Reports. 2002; 22(2):251–266. [PubMed: 12428903]
22. Terato K, Hasty KA, Reife RA, Cremer MA, Kang AH, Stuart JM. Induction of arthritis with monoclonal antibodies to collagen. J Immunol. 1992; 148(7):2103–2108. [PubMed: 1545120]
23. Achnyder A, Huwyler J. Drug transport to brain with targeted liposomes. J of the Am Soc for Exp Neuro Therapeutics. 2005; 2:99–107.
24. Achnyder A, Krahenbuhl S, Torok M, Drewe J, Huwyler J. Targeting of skeletal muscle in vitro using biotinylated immunoliposomes. Biochem J. 2004; 377:61–67. [PubMed: 14516278]
25. Huwyler J, Yang J, Pardridge WM. Receptor mediated delivery of daunomycin using immunoliposomes: pharmacokinetics and tissue distribution in the rat. J Pharmacol Exp Ther. 1997; 282(3):1541–1546. [PubMed: 9316870]
26. Huwyler J, Wu D, Pardridge WM. Brain drug delivery of small molecules using immunoliposomes. Proc Natl Acad Sci. 1996; 93(24):14164–14169. [PubMed: 8943078]
27. Olson F, Hunt CA, Szoka FC, Vali WJ, Papahadjopoulos D. Preparation of liposomes of defined size distribution by extrusion through polycarbonate membranes. Biochim Biophys Acta. 1979; 557(1):9–23. [PubMed: 95096]
28. Rongen HAH, Bult A, van Benneekom WP. Liposomes and immunoassays. J of Immunological Methods. 1997; 204:105–133. [PubMed: 9212829]
29. Szoka F, Olson F, Heath T, Vail W, Mayhew E, Papahadjopoulos D. Preparation of unilamellar liposomes of intermediate size (0.1–0.2 um) by a combination of reverse phase evaporation and extrusion through polycarbonate membranes. Biochim Biophys Acta. 1980; 601(3):559–571. [PubMed: 6251878]
30. Harris, ED, Jr. Pathogenesis of Rheumatoid Arthritis. In: Kelley, WNea, editor. Textbook of Rheumatology. W. B. Saunders; Philadelphia: 1985. p. 886-903.
31. Mankin HJ, Dorfman H, Lippiello L, Zarins A. Biochemical and metabolic abnormalities in articular cartilage from osteo-arthritic human hips. II. Correlation of morphology with biochemical and metabolic data. J Bone Joint Surg. 1971; 53:523–537. [PubMed: 5580011]
32. Moghimi SM, Szebeni J. Stealth liposomes and long circulating nanoparticles: critical issues in pharmacokinetics, opsonization and protein-binding properties. Prog in Lipid Res. 2003; 42:463–478. [PubMed: 14559067]
33. Torchilin, VP.; Weissig, V. Liposomes, Practical Approach. 2. Oxford University Press; 2003.
34. Zhang L, Granick S. How to stabilize phospholipids liposomes. Nano Letters. 2006; 6(4):694–698. [PubMed: 16608266]
35. Liu D, Mori A, Huang L. Large liposomes containing ganglioside GM1 accumulate effectively in spleen. Biochem Biophys Acta. 1991; 1066:159–165. [PubMed: 1854781]
36. Liu D, Mori A, Huang L. Role of liposome size and RES blockade in controlling biodistribution and tumor uptake of GM-1 containing liposomes. Biochem Biophys Acta. 1992; 1104:95–101. [PubMed: 1550858]

37. Torchilin VP. Recent advances with liposomes as pharmaceutical carriers. Nature Reviews. 2005; 4:145–160.
38. Torchilin VP. Multifunctional and stimuli-sensitive pharmaceutical nanocarriers. Eur J Pharm Biopharm. 2009; 71:431–444. [PubMed: 18977297]
39. Vojta A, Scheuring J, Neumaier N, Mirus O, Weinkauf S, Schleiff E. Determination of liposome size: A tool for protein reconstitution. Analytical Biochem. 2005; 347:24–33.
40. Smith GN Jr. The role of collagenolytic matrix metalloproteinases in the loss of articular cartilage in osteoarthritis. Front Biosci. 2006; 11:3081–3095. [PubMed: 16720377]
41. Vanniasinghe A, Bender V, Manolios N. The potential of liposomal drug delivery for the treatment of inflammatory arthritis. J Semi Arthritis Rheum. 2009; 39:182–196.
42. Tanaka H, Sugita T, Yasunaga Y, Shimose S, Deie M, Kubo T, Murakami T, Ochi M. Efficiency of magnetic liposomal transforming growth factor-beta 1 in the repair of articular cartilage defects in a rabbit model. J biomed Mat Res. 2005; 73A:255–263.
43. Ballock RT, Heydemann A, Wakefield LM, Flanders KC, Roberts AB, Sporn MB. Inhibition of the chondrocyte phenotype by retinoic acid involves upregulation of metalloprotease genes independent of TGF-beta. J Cell Physiol. 1994; 159(2):340–346. [PubMed: 8163572]
44. Pujol JP, Galera P, Redini F, Mauviel A, Loyau G. Role of cytokines in osteoarthritis: comparative effects of interleukin 1 and transforming growth factor-beta on cultured rabbit articular chondrocytes. J Rheumatol Suppl. 1991; 27:76–97. [PubMed: 2027137]
45. Shlopov BV, Gumanovskaya ML, Hasty KA. Autocrine regulation of collagenase 3 (matrix metalloproteinase 13) during osteoarthritis. Arthritis Rheum. 2000; 43(1):195–205. [PubMed: 10643716]
46. Shlopov BV, Smith GN Jr, Cole AA, Hasty KA. Differential patterns of response to doxycycline and transforming growth factor beta1 in the down-regulation of collagenases in osteoarthritic and normal human chondrocytes. Arthritis Rheum. 1999; 42(4):719–727. [PubMed: 10211886]
47. Matrisian LM. The matrix-degrading metalloproteinases. Bioessays. 1992; 14(7):455–463. [PubMed: 1445287]
48. Matrisian LM, Ganser GL, Kerr LD, Pelton RW, Wood LD. Negative regulation of gene expression by TGF-beta. Mol Reprod Dev. 1992; 32(2):111–120. [PubMed: 1637549]

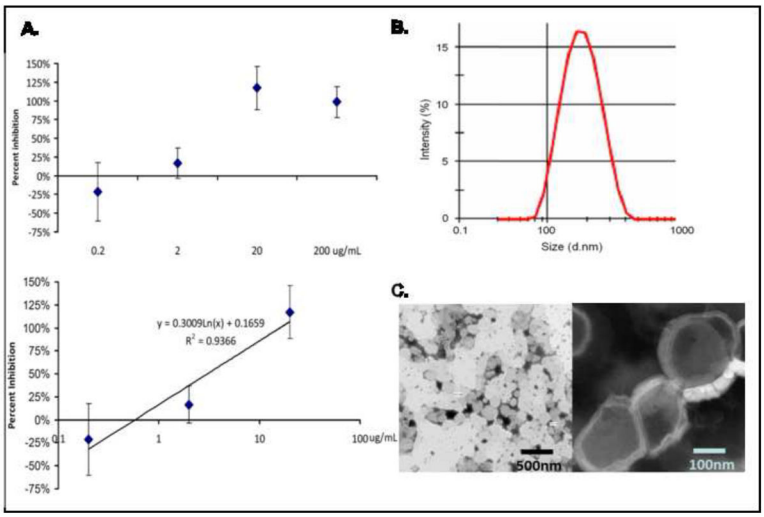

Figure 1. Characterization of immuno-liposomes

(A) Kinetics of binding to type II collagen. To determine the binding characteristics of the MAbCII-coupled liposomes, the liposomes were pre-incubated with a known concentration of purified type II collagen overnight, then incubated with a collagen II coated ELISA plate. Liposomes bound to type II collagen were detected with an alkaline phosphatase coupled secondary antibody, using a PNPP substrate. Using a logarithmic regression curve, it was determined that the K_d was 3.0μg/mL, similar to the value observed for the free antibody (1.7μg/mL). (B) Size distribution by DLS. Analysis by DLS showed only one population with a Z-average of 200nm for the immuno-liposomes mixture. (C) Characterization by SEM. The DOPC liposomes are uniform in size with a range of diameter of 150–250 nm. After coupling to antibody, the shape and size of the liposomes remains constant (left side of C). The liposomes were multilamellar structures (right side of C) with 1–4 layers.

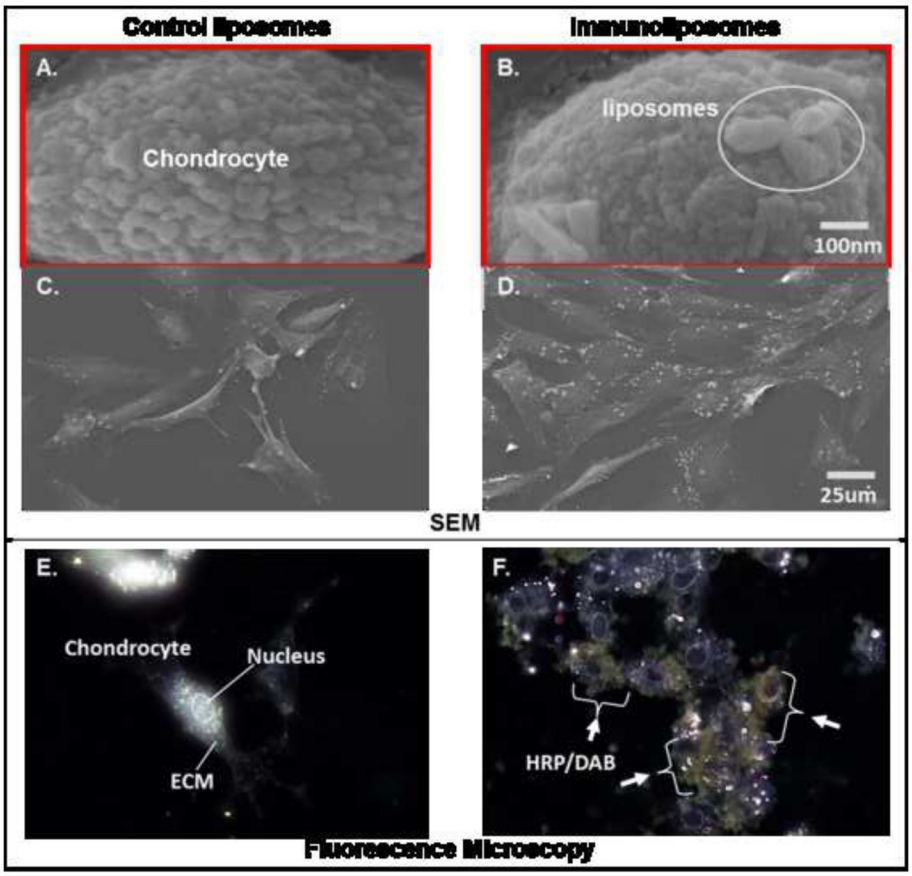

Figure 2. Localization of immuno-liposomes on cultured chondrocytes by SEM & fluorescence microscopy

Images of SEM (A, B, C and D); (A and C) Control group: Cultured chondrocytes were treated with control liposomes that were not coupled to antibody, (A is 500x magnitude, C is 12800x magnitude); (B and D) Experimental group: cultured chondrocytes were treated with the immuno-liposomes which were conjugated to CII antibody, (B is 500x magnitude, C is 12800x magnitude); Images of fluorescence microscopy of cultured chondrocytes incubated with control and immuno-liposomes filled with peroxidase and stainined with DAB substrate (E and F); (E) Control group: control liposomes showed no staining with DAB substrate, (F) Experimental group: HRP encapsulated in immuno-liposomes showed localization in proximity to chondrocytes

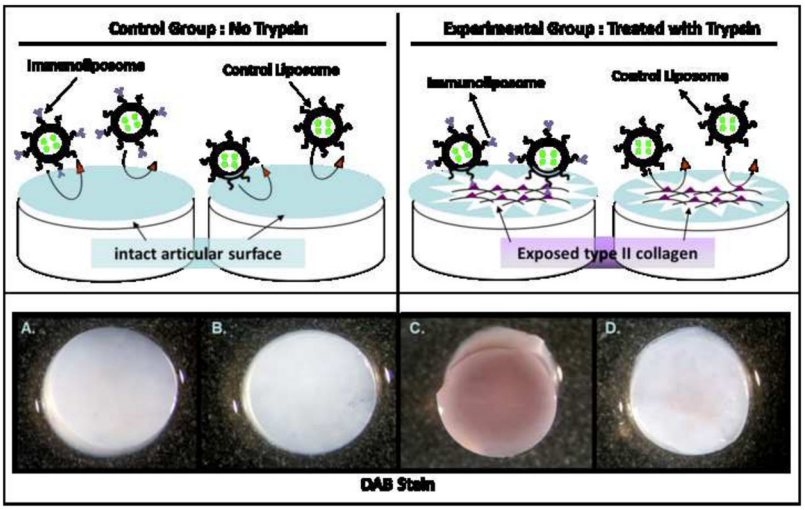

Figure 3. in vitro model of creating articular cartilage lesions with trypsin digestion and exclusive localization of immuno-liposomes to damaged cartilage explants

Articular cartilage explants were incubated with (C and D) trypsin to mimic a damaged cartilage tissue, or without (A and B) trypsin for intact tissue, then incubated for 1 hr with peroxidase-filled nanosomes coupled to type II collagen antibody (immuno-liposomes, A and C) or peroxidase-filled liposomes alone (control liposomes, B and D). After a secondary punch with a 4mm biopsy punch to remove the sides that were mechanically damaged from the initial harvesting, the cartilage tissues were incubated with the peroxidase substrate DAB. Only the articular cartilage treated with trypsin (C) binds to the immuno-liposomes.

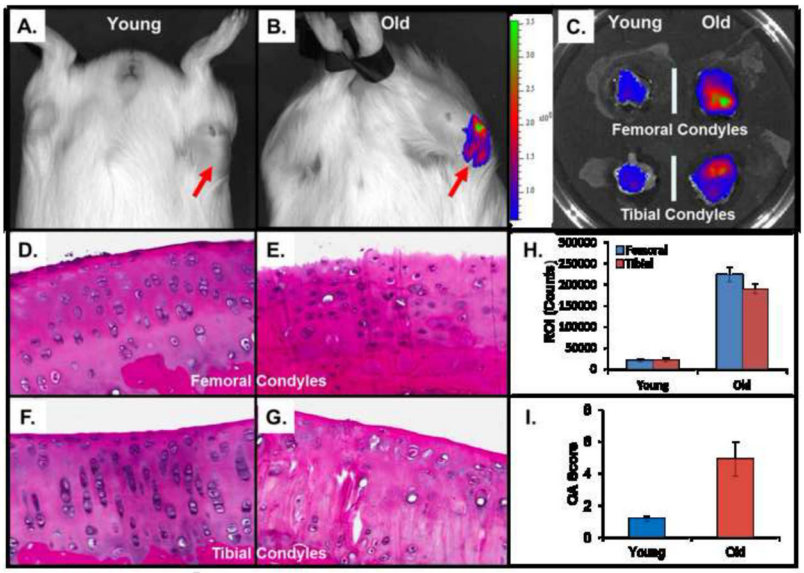

Figure 4. IVIS imaging of DH guinea pigs intravenously injected with MAbCII liposome

Animals were IVIS imaged at 24 hours after injection. (A and B) IVIS scan images of young and older guinea pig (n=12 for each age group). (C) IVIS imaging of cartilages from dissected knee joints; (H) total integrated intensity of fluorescence (ROI) in femoral and tibial condyles was quantitated and normalized using imaging software. (D, E, F and G) Histopathology of Hematoxylin and Eosin (H&E) stained sections of articular knee cartilage from young & old GP showing regional variation in morphology. Tibial condyles were decalcified, embedded and 60 H&E-stained sections from each specimen were prepared with a constant interval of 100 μm to survey the articular cartilage. (I) These sections were then graded by an observer using a modified Mankin scale (normal; grade 0–2, slight; grade 3–5, moderate; grade 6–8 and severe; grade 9–11).